

Strain effect on band offsets at pseudomorphic InAs/GaAs heterointerfaces characterized by x-ray photoemission spectroscopy

K. Hirakawa, Y. Hashimoto, K. Harada, and T. Ikoma

Institute of Industrial Science, University of Tokyo, 7-22-1 Roppongi, Minato-ku, Tokyo 106, Japan

(Received 1 November 1990; revised manuscript received 21 March 1991)

We studied heterojunction band offsets at highly strained InAs/GaAs (100) heterointerfaces, using *in situ* x-ray photoemission spectroscopy with an emphasis on the effects of strain. Two extreme cases are examined: an InAs layer pseudomorphically grown on a GaAs substrate (type I); a GaAs layer grown on an InAs substrate (type II). It was found that the energy difference between In 4*d* and Ga 3*d* core levels in InAs/GaAs heterostructures depends only slightly on the in-plane lattice constant: 1.64 eV for type I and 1.60 eV for type II. However, the valence-band offsets $\Delta E_V [\equiv E_V(\text{InAs}) - E_V(\text{GaAs})]$, which are deduced by theoretically taking into account the effects of strain on the core-level energies relative to the valence-band maxima as well as on a splitting of the valence-band maxima, are very different: 0.53 eV for type I and -0.16 eV for type II. This clearly indicates a large effect of strain on the valence-band offset (~ 0.7 eV) in this system.

I. INTRODUCTION

The heterojunction band offset (HBO) is one of the most important parameters that determine the performance of semiconductor heterostructure devices. In lattice-matched heterojunction systems, the HBO is determined with an accuracy of ± 0.05 eV by x-ray photoemission spectroscopy (XPS) as well as by electrical and optical methods.^{1,2}

Recently, InAs/GaAs short-period superlattices have attracted much attention for the possibility to replace a disordered $\text{In}_x\text{Ga}_{1-x}\text{As}$ alloy.³ In spite of their importance, only a few experiments have been done to determine the InAs/GaAs HBO experimentally. A main difficulty arises from the fact that this system has about 7% lattice mismatch and the critical thickness for a generation of misfit dislocations is as thin as 2 monolayers (ML).⁴ This makes it very difficult to determine HBO's accurately by the conventional electrical and/or optical methods that have been successfully applied to lattice-matched systems.

Kowalczyk *et al.* reported the valence-band offset, ΔE_V , at InAs/GaAs to be 0.17 eV from their XPS measurements.⁵ However, their measurement was carried out on an InAs/GaAs single heterojunction with a 20-Å-thick InAs layer, which is much thicker than the critical thickness for dislocation generation. Hence, the lattice strain is considered to be relaxed in their samples. Therefore, to specify the strain condition and clarify its effects on the HBO at InAs/GaAs heterointerfaces, the structural parameters of the specimen must be carefully chosen.

In this work, we studied the HBO's at pseudomorphic InAs/GaAs (100) interfaces by *in situ* XPS measurements with an emphasis on the strain effects. The quantities that can be directly measured by XPS are the energy difference, ΔE_{CL} , between In 4*d* and Ga 3*d* core levels in InAs/GaAs heterostructures and the core-level binding

energies relative to the respective valence-band maxima (VBM), $E_{\text{Ga } 3d}^V$ and $E_{\text{In } 4d}^V$, in unstrained bulk GaAs and InAs. To deduce ΔE_V , we took into account the strain-induced shifts of the core-level binding energies relative to the VBM by using the theory developed by Enderlein and Harrison.⁶ ΔE_V thus determined is found to be strongly dependent on the in-plane lattice constant, although the measured ΔE_{CL} is only slightly dependent on it. The results are compared with recent experimental and theoretical results.^{5,7-10}

II. THEORETICAL BACKGROUND

Figure 1 shows a schematic energy-band diagram at the InAs/GaAs heterointerface. The valence-band offset defined by $\Delta E_V \equiv E_V(\text{InAs}) - E_V(\text{GaAs})$ is given by⁵

$$\Delta E_V = -E_{\text{Ga } 3d}^V + E_{\text{In } 4d}^V + \Delta E_{CL} . \quad (1)$$

$E_{\text{Ga } 3d}^V$, $E_{\text{In } 4d}^V$, and also ΔE_{CL} are considered to be affected by lattice strain.¹¹ We will consider two extreme cases for strained InAs/GaAs heterostructures; one is the case where an InAs layer is pseudomorphically grown on a GaAs substrate (InAs strained case; type I), and the other is the case where a GaAs layer is pseudomorphically grown on an InAs substrate (GaAs strained case; type II). We will rewrite Eq. (1) as the following in order to express the strain effects explicitly:

$$\Delta E_V = -E_{\text{Ga } 3d}^{V0} + E_{\text{In } 4d}^{VS} + \Delta E_{CL}^I \quad (\text{type I}) , \quad (2)$$

$$\Delta E_V = -E_{\text{Ga } 3d}^{VS} + E_{\text{In } 4d}^{V0} + \Delta E_{CL}^{II} \quad (\text{type II}) . \quad (3)$$

Here, the superscript *S* denotes the values for strained layers and 0 the unstrained bulk values. ΔE_{CL}^I and ΔE_{CL}^{II} can be directly determined by XPS measurements on pseudomorphically grown InAs/GaAs heterojunctions (as described in Sec. III). $E_{\text{Ga } 3d}^{V0}$ and $E_{\text{In } 4d}^{V0}$ can be obtained from XPS spectra on unstrained bulk GaAs and InAs, respectively. However, it is very difficult to deter-

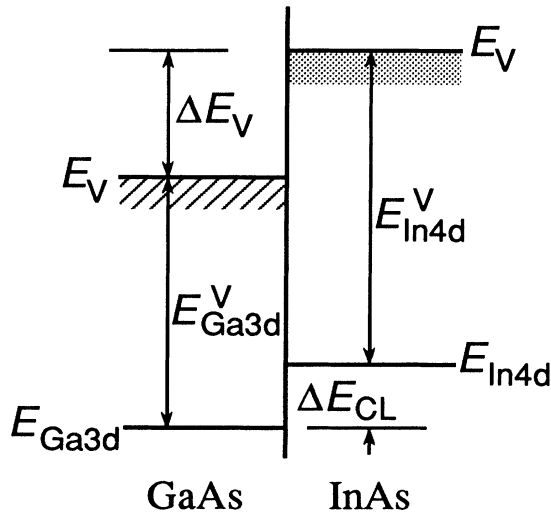


FIG. 1. A schematic energy-band diagram at an InAs/GaAs heterojunction.

mine $E_{\text{Ga}3d}^{\text{VS}}$ and $E_{\text{In}4d}^{\text{VS}}$ experimentally. In the previous work,⁵ $E_{\text{Ga}3d}^{\text{VS}}$ and $E_{\text{In}4d}^{\text{VS}}$ were replaced with the unstrained values. However, this approximation is not always correct. Therefore, in order to determine the HBO's in strained InAs/GaAs systems, we estimated $E_{\text{Ga}3d}^{\text{VS}}$ and $E_{\text{In}4d}^{\text{VS}}$ by the following theoretical consideration and also by the direct XPS measurements on strained GaAs layers (see Sec. III B).

The biaxial strain associated with pseudomorphic epitaxy can be decomposed into the hydrostatic part and the uniaxial part (see Appendix A). Van de Walle and Martin have theoretically shown that the energy difference between the centroid of the valence-band maximum (CVBM) and the core level is influenced only by the hydrostatic part and that the uniaxial part splits the valence bands around the centroid.¹² By taking into account these strain effects, the energy-band diagrams are shown in Fig. 2 for type-I and -II systems.

The hydrostatic part of the strain shifts the CVBM relative to the core levels. $E_{\text{In}4d}^{\text{CVS}}$ and $E_{\text{Ga}3d}^{\text{CVS}}$ denote the shifted CVBM measured from the In 4d core level in strained InAs and that measured from the Ga 3d core level in strained GaAs, respectively, which are different from the unstrained bulk values of $E_{\text{In}4d}^{\text{CV}0}$ for InAs and $E_{\text{Ga}3d}^{\text{CV}0}$ for GaAs. Furthermore, the uniaxial part of the strain splits the threefold-degenerate VBM into heavy-hole (hh), light-hole (lh), and spin-orbit split-off (SO) bands around the CVBM. The splittings of hh and lh bands relative to the CVBM, E_{hh}^u and E_{lh}^u , can be estimated by using appropriate deformation-potential constants. $E_{\text{In}4d}^{\text{VS}}$ and $E_{\text{Ga}3d}^{\text{VS}}$ are then obtained by $E_{\text{In}4d}^{\text{CVS}} + E_{\text{hh,lh}}^u$ and $E_{\text{Ga}3d}^{\text{CVS}} + E_{\text{hh,lh}}^u$ for hh and lh bands, respectively.

First, let us evaluate the effects of the hydrostatic part of strain. Because of the core-hole relaxation effect during XPS measurements, the measured binding energy of the core electrons relative to the CVBM, $E_{\text{CL}}^{\text{CV}}$, is different

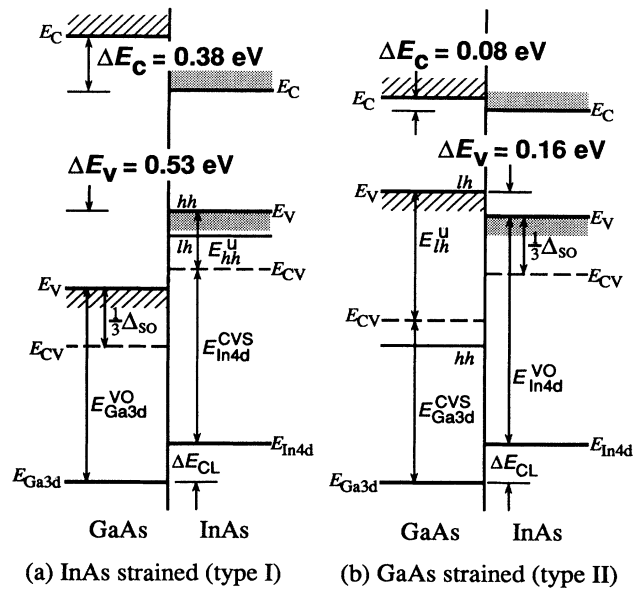


FIG. 2. Band lineups at strained type-I and type-II heterointerfaces.

from the unperturbed binding energy. This shift (the so-called “final-state effect”) can be treated by using a Born-Haber cycle. Using the tight-binding (TB) theory with universal parameters and also using the $Z + 1$ approximation, the unstrained $E_{\text{CL}}^{\text{CV}}$ is given by⁶

$$E_{\text{CL}}^{\text{CV}0} = \Delta E_{\text{bond}} + E_{\text{CV}} + \Delta E_{\text{met}} + I_{\text{core}}. \quad (4)$$

Here, ΔE_{bond} and ΔE_{met} denote the differences in the bond formation energy and the metallization correction between the initial and final states, respectively. E_{CV} denotes the theoretical CVBM, and I_{core} denotes the core-level ionization energy in a free atom (see Appendix B for details). Under the hydrostatic strain with an isotropic strain component of e_h (see Appendix A), we can calculate the binding energy of a core electron in the same manner and obtain $E_{\text{CL}}^{\text{CVS}}$. Because of the $Z + 1$ approximation and the TB approach, the absolute values of the calculated $E_{\text{CL}}^{\text{CVS}}$ and $E_{\text{CL}}^{\text{CV}0}$ have uncertainties, but the calculated strain-induced shifts, $(E_{\text{CL}}^{\text{CVS}} - E_{\text{CL}}^{\text{CV}0})$, are reliable. Therefore, we will use the following approximation:

$$E_{\text{CL}}^{\text{CVS}} \equiv E_{\text{CL}}^{\text{CV}0}(\text{expt}) + [E_{\text{CL}}^{\text{CVS}}(\text{theor}) - E_{\text{CL}}^{\text{CV}0}(\text{theor})] \quad (5)$$

with

$$E_{\text{CL}}^{\text{CV}0}(\text{expt}) = E_{\text{CL}}^{\text{V}0}(\text{expt}) - \frac{1}{3}\Delta_{\text{s.o.}}, \quad (6)$$

where (expt) and (theor) denote the quantities obtained experimentally and theoretically, respectively. $\Delta_{\text{s.o.}}$ is the spin-orbit splitting energy ($\Delta_{\text{s.o.}} = 0.38$ eV for InAs and $\Delta_{\text{s.o.}} = 0.34$ eV for GaAs). The calculated strain-induced shifts, $[E_{\text{CL}}^{\text{CVS}}(\text{theor}) - E_{\text{CL}}^{\text{CV}0}(\text{theor})]$, are tabulated in Table I.

The uniaxial strain splits the threefold-degenerate

TABLE I. Calculated energies for strained GaAs and InAs (in eV). The subscript *CL* represents the Ga 3*d* or In 4*d* core levels in GaAs or InAs, respectively. To obtain E_{CL}^{CVS} by Eq. (5), we used the values of E_{CL}^{V0} measured by XPS, which are tabulated in Table II.

	$E_{CL}^{CVS}(\text{theor}) - E_{CL}^{V0}(\text{theor})$	E_{CL}^{CVS}	E_{hh}^u	E_{lh}^u	E_{CV}^{CS}
InAs (type I)	0.02	17.25	0.39	0.18	0.90
GaAs (type II)	-0.11	18.53	-0.17	0.59	0.86

VBM into hh, lh, and SO bands. With the deformation-potential constant b ,¹³ the splittings of the heavy- and light-hole bands relative to the CVBM, E_{hh}^u and E_{lh}^u are, respectively, given by^{11,12,14}

$$E_{hh}^u = \frac{1}{3}\Delta_{s.o.} - \frac{1}{2}\delta E_{001}, \quad (7)$$

$$E_{lh}^u = -\frac{1}{6}\Delta_{s.o.} + \frac{1}{4}\delta E_{001} + \frac{1}{2}(\Delta_{s.o.}^2 + \Delta_{s.o.}\delta E_{001} + \frac{9}{4}\delta E_{001}^2)^{1/2}, \quad (8)$$

with

$$\delta E_{001} = 2b(a_{\perp}/a_0 - a_{\parallel}/a_0). \quad (9)$$

Here, a_0 denotes the bulk lattice parameter, and a_{\perp} and a_{\parallel} denote the strained lattice parameter parallel and normal to the growth direction, respectively. In uniaxially expanded (biaxially compressed) InAs, the VBM is the heavy-hole band, while in uniaxially compressed (biaxially expanded) GaAs it is the light-hole band.

The conduction band relative to the CVBM, E_{CV}^{CS} , can be calculated by using the hydrostatic deformation-potential constant a ,¹³ as follows:¹⁴

$$E_{CV}^{CS} = E_g^0 + \frac{1}{3}\Delta_{s.o.} + a \left[\frac{a_{\parallel}^2 a_{\perp}}{a_0^3} - 1 \right]. \quad (10)$$

Here, E_g^0 denotes the direct band gap for unstrained bulk material. These values are also tabulated in Table I.

III. SAMPLES AND XPS MEASUREMENTS

A. Core-level energy distance

All the samples used in these experiments were grown by molecular-beam epitaxy (MBE). In order to investigate the strain effects on HBO's, we prepared unstrained bulk GaAs and InAs and two types of heterostructures (HS's), i.e., an InAs layer grown on a GaAs substrate (type-I HS) and a GaAs layer grown on an InAs substrate (type-II HS). To avoid the generation of misfit dislocations, the thickness of the heterojunction overlayers was set to be as thin as 2 ML. However, the XPS signals from such thin overlayers are strongly affected by the surface chemical shift. To eliminate this ambiguity, we grew capping layers on the strained thin layers; i.e., 5-ML-thick GaAs layers for type-I structures and 5-ML-thick InAs layers for type-II structures. Thus, the samples measured in these experiments are double heterostructures; i.e., GaAs/InAs/GaAs structures (type-I HS) and reversed InAs/GaAs/InAs structures (type-II HS). For type-I HS, a 1- μm -thick Si-doped GaAs buffer layer,

a 2-ML-thick undoped InAs strained interlayer, and a 5-ML-thick GaAs capping layer were successively grown on a Si-doped GaAs(100) substrate. For a type-II HS, a 1- μm -thick undoped InAs buffer, a 2-ML-thick undoped GaAs interlayer, and a 5-ML-thick undoped InAs capping layer were grown on an undoped *n*-type InAs(100) substrate.

Clean mirror surfaces were obtained at substrate temperatures around 450°C under an As-rich condition. The growth rate was calibrated by the reflection high-energy electron-diffraction (RHEED) oscillation. The uncertainty in film thickness is less than 10%. RHEED patterns were photographically recorded to ensure that the lattice relaxation did not occur in these samples.

The samples were transferred to the XPS chamber via the ultrahigh vacuum ($< 10^{-10}$ Torr) transfer tube immediately after the growth. XPS measurements were performed with a monochromatic Al $K\alpha$ x-ray source ($h\nu = 1486.6$ eV). The analyzer pass energy was set to be 20 eV. The instrumental resolution under this condition is about 0.7 eV.

First, we measured $E_{Ga\ 3d}^{V0}$ and $E_{In\ 4d}^{V0}$ on MBE-grown unstrained bulk GaAs and InAs samples, respectively. In the XPS spectra the background intensity, which is proportional to the integrated peak intensity, was subtracted from each core-level spectrum.² Here, we simply define the peak position of each core level as the midpoint of the two energies at which the intensity is half of the maximum intensity.^{2,15} To determine the energy position of the VBM, E_V , the theoretical densities of states¹⁶ for GaAs and InAs broadened by the instrumental line shape were fit to the XPS spectra around the VBM.² The obtained values of $E_{Ga\ 3d}^{V0}$ and $E_{In\ 4d}^{V0}$ are tabulated in Table II.

The XPS spectra were then measured on type-I and -II HS's to determine ΔE_{CL}^I and ΔE_{CL}^{II} . Typical XPS spectra are shown in Fig. 3. We made three independent experiments for each type of structures to assure the accuracy. The least-squares fitting by the Ga 3*d* and In 4*d* core-level spectra taken on bulk GaAs and InAs samples, respectively, was used to separate the two closely spaced

TABLE II. Energy differences measured by XPS.

Sample	Energy	Value (eV)
InAs/GaAs (type-I HS)	ΔE_{CL}^I	1.64±0.02
GaAs/InAs (type-II HS)	ΔE_{CL}^{II}	1.60±0.02
Bulk GaAs	$E_{Ga\ 3d}^{V0}$	18.75±0.05
Bulk InAs	$E_{In\ 4d}^{V0}$	17.36±0.05

core levels.⁵ The ΔE_{CL} 's thus determined were 1.64 ± 0.02 eV and 1.60 ± 0.02 eV for type-I and -II samples, respectively. This result shows that ΔE_{CL} depends only slightly on the in-plane lattice constant.

B. Strain-induced shift in the core-level binding energy

In order to check the validity of our theoretical approach to calculate the core-level binding energy relative to the VBM, $E_{CL}^{CVS} - E_{CL}^{CV0}$, the strain-induced shift in the Ga 3d level binding energy in GaAs was systematically measured as a function of the in-plane lattice constants

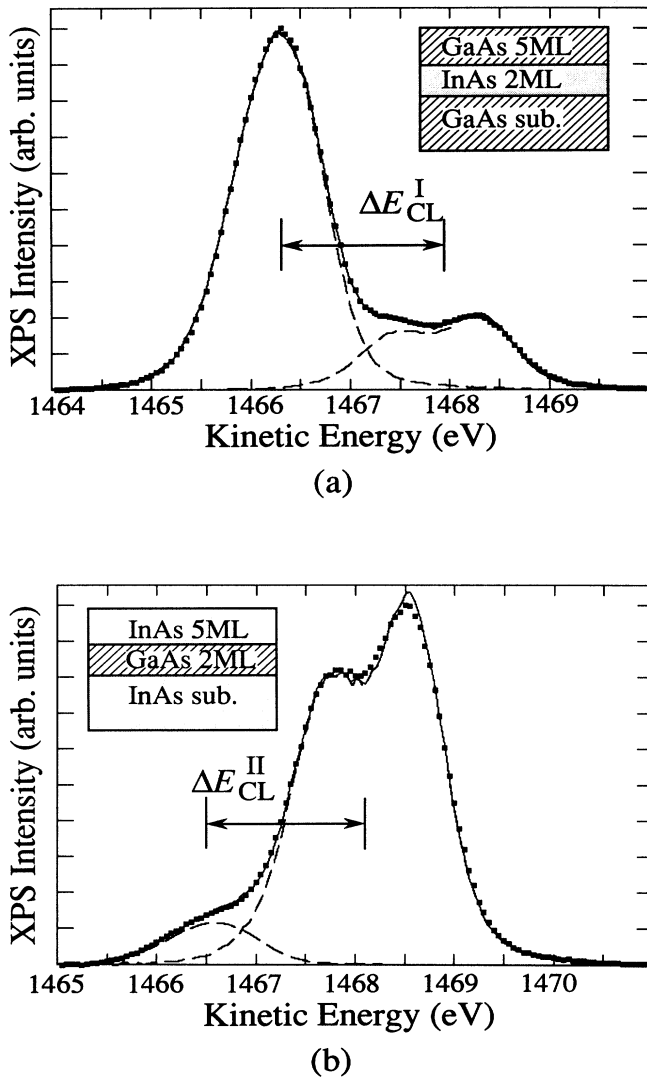


FIG. 3. Typical XPS spectra measured on (a) type-I and (b) type-II samples. The backgrounds are subtracted as described in the text. The dots are the XPS data and the solid lines are fitting curves by using the Ga 3d and In 4d core-level spectra (dashed lines), which are obtained from XPS measurements on respective bulk materials. The insets show the sample structures.

a_{\parallel} .¹⁷ Each of the samples, which consists of a 1- μm -thick $\text{In}_x\text{Ga}_{1-x}\text{As}$ buffer layer ($x=0\sim 0.37$) and a 50- \AA -thick GaAs capping layer, was grown on an n^+ -GaAs substrate by MBE and *in situ* XPS measurements were performed. The in-plane lattice constant of the strained GaAs overlayer was determined by x-ray-diffraction measurements on the lattice constant in the $\text{In}_x\text{Ga}_{1-x}\text{As}$, to which the strained GaAs overlayer matches its a_{\parallel} unless the lattice relaxation occurs in the overlayer. The 50- \AA thick GaAs overlayer is thicker than the photoelectron escape depth (~ 25 \AA) and dominates the XPS signal from these samples. The energy positions of the Ga 3d level and the VBM are determined by comparing the measured XPS spectrum with that of unstrained GaAs.

In Fig. 4, the shift in the Ga 3d core-level binding energy is plotted as a function of the in-plane lattice constant a_{\parallel} . The measured binding energy increases gradually by approximately 50 meV when a_{\parallel} increases from 5.65 \AA (equilibrium GaAs lattice constant) to 5.73 \AA . The solid curve in Fig. 4 denotes the theoretical result obtained by substituting a_{\parallel} into Eqs. (5)–(9) and agrees well with experimental results when $a_{\parallel} < 5.73$ \AA . The discrepancy observed when a_{\parallel} exceeds 5.73 \AA is due to the generation of misfit dislocations and resulting lattice relaxations, since the critical thickness is lower than 50 \AA when $a_{\parallel} > 5.75$ \AA . This experiment strongly supports the validity of our theoretical approach by Eqs. (5)–(9) in predicting the strain effect at InAs/GaAs heterojunctions.

IV. DERIVATION OF BAND OFFSETS AND DISCUSSIONS

$E_{\text{In } 4d}^{CVS}$ and $E_{\text{Ga } 3d}^{CVS}$ are obtained by substituting into Eqs. (5) and (6) the calculated energy shifts [$E_{CL}^{CVS}(\text{theor}) - E_{CL}^{CV0}(\text{theor})$] and the measured values of $E_{\text{In } 4d}^{V0}$ and $E_{\text{Ga } 3d}^{V0}$. Then, by combining these values with ΔE_{CL}^I and ΔE_{CL}^{II} , the offsets of the CVBM, $\Delta E_{CV} [\equiv E_{CV}(\text{InAs}) - E_{CV}(\text{GaAs})]$, are obtained as

$$\Delta E_{CV} = -E_{\text{Ga } 3d}^{CV0} + E_{\text{In } 4d}^{CVS} + \Delta E_{CL}^I \quad (\text{type I}), \quad (11)$$

$$\Delta E_{CV} = -E_{\text{Ga } 3d}^{CVS} + E_{\text{In } 4d}^{CV0} + \Delta E_{CL}^{II} \quad (\text{type II}). \quad (12)$$

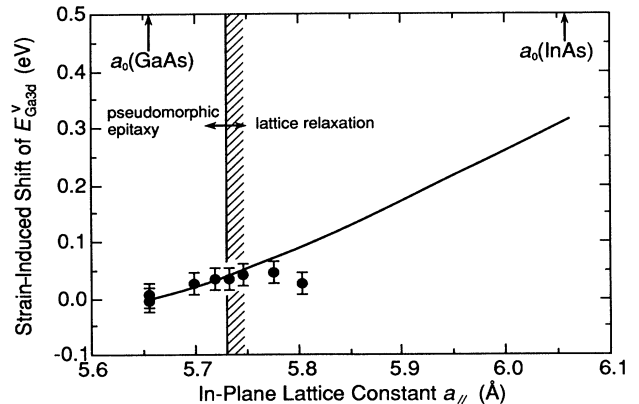


FIG. 4. Shift in the Ga 3d core-level binding energy relative to the VBM plotted as a function of the in-plane lattice constant a_{\parallel} .

The determined ΔE_{CV} 's are 0.25 and 0.30 eV for type-I and -II HS's, respectively. Furthermore, by taking into account the effect of the uniaxial strain as described in Sec. II, all the parameters that define the energy-band diagrams are determined, as listed in Table III. The resulting band lineups are shown in Fig. 2. A ΔE_V of 0.53 eV and a conduction-band offset, $\Delta E_C[\equiv E_C(\text{InAs}) - E_C(\text{GaAs})]$, of -0.38 eV are obtained for the type-I structure. In this case, both hh and lh bands in InAs are above the VBM in GaAs. The VBM in the strained InAs is a hh band. In contrast, a characteristic band alignment is expected for the type-II structure, where the lh (hh) band in the strained GaAs layer is higher (lower) than the VBM in the InAs by 0.16 eV (0.60 eV) and the conduction-band offset is 0.08 eV.

Kowalczyk *et al.* reported ΔE_V of 0.17 eV determined by XPS measurements on an InAs/GaAs single heterojunction.⁵ The discrepancy between their result and ours is considered to be due to the lattice relaxation in their sample, since the InAs layer in their sample is much thicker than the critical thickness for dislocation generation. On the other hand, Menéndez *et al.* predicted a much larger ΔE_{CV} (0.49 ± 0.1 eV for type I) by extrapolating the value obtained by light-scattering experiments on $\text{In}_{0.05}\text{Ga}_{0.95}\text{As}/\text{GaAs}$ quantum wells.⁷ This is even larger than our results. Although the origin of this discrepancy is not clear at present, it is uncertain whether such a simple extrapolation can give a correct value.

Cardona and Christensen predicted $\Delta E_V = 0.52$ eV for type I from their dielectric midgap energy theory,⁸ which is in excellent agreement with our ΔE_V (0.53 eV). On the other hand, Priester, Allan and Lannoo theoretically predicted ΔE_{CV} to be 0.09 eV for type I and 0.19 eV for type II by self-consistent tight-binding calculations,⁹ and Taguchi and Ohno obtained $\Delta E_{CV} = 0.02$ eV for type I and 0.01 eV for type II by the *ab initio* self-consistent pseudopotential method.¹⁰ Our values of ΔE_{CV} (0.27 eV for type I and 0.36 eV for type II) are much larger than these theoretical predictions, calling for further refinement in the theories.

V. CONCLUSIONS

The energy-band lineups at strained InAs/GaAs heterojunctions were studied by *in situ* XPS measure-

TABLE III. Determined band offsets (in eV). ΔE_{CV} , ΔE_{hh} , and ΔE_{lh} denote the offsets in the CVBM, the heavy-hole band, and the light-hole band, respectively. ΔE_V represents the offset of VBM. ΔE_C denotes the conduction-band offset at the Γ point defined by $\Delta E_C \equiv E_C(\text{InAs}) - E_C(\text{GaAs})$.

	InAs strained case (type I)	GaAs strained case (type II)
ΔE_{CV}	0.25	0.30
ΔE_{hh}	0.53	0.60
ΔE_{lh}	0.32	-0.16
ΔE_V	0.53	-0.16
ΔE_C	-0.38	-0.08

ments on InAs/GaAs heterostructures grown on GaAs substrates (type I) and InAs substrates (type II) by MBE. It was found that the core-level energy difference ΔE_{CL} between In 4*d* and Ga 3*d* levels in InAs/GaAs heterostructures depends only slightly on the in-plane lattice constant. By taking into account theoretically the strain-induced shifts of the core-level binding energies relative to the VBM, the offset of the centroid of the VBM, ΔE_{CV} , is determined to be 0.25 eV for type I and 0.30 eV for type II. Furthermore, by adding the splitting of the VBM due to the uniaxial part of strain, the valence-band offset ΔE_V is determined to be 0.53 and -0.16 eV for type I and II, respectively, demonstrating very large effects of strain on the band lineups. The energy-band diagrams discussed here are essential to predict optical and electrical properties of short-period superlattices and very thin quantum wells.¹⁸

ACKNOWLEDGMENTS

We are grateful to T. Saito and M. Noguchi for valuable discussions. We thank Professor T. Homma for extending us the use of the x-ray diffractometer. This work is partly supported by a Grant-in-Aid from the Ministry of Education, Science, and Culture, Japan, by the Foundation for Promotion of Material Science and Technology of Japan (MST), and also by the Industry-University Joint Research Program "Mesoscopic Electronics."

APPENDIX A

The strain components arising from the pseudomorphic epitaxy are given by

$$e_{xx} = e_{yy} = \left[\frac{a_{\parallel}}{a_0} - 1 \right], \quad (\text{A1})$$

$$e_{zz} = \left[\frac{a_{\perp}}{a_0} - 1 \right], \quad (\text{A2})$$

where a_0 denotes the bulk lattice parameter, and a_{\parallel} and a_{\perp} denote the strained lattice parameter parallel and normal to the interface, respectively. By using the elastic compliance constants S_{11} and S_{12} , e_{zz} is expressed as

$$e_{zz} = \frac{2S_{12}}{S_{11} + S_{12}} \left[\frac{a_{\parallel}}{a_0} - 1 \right]. \quad (\text{A3})$$

This biaxial strain can be decomposed into the hydrostatic and uniaxial components as

$$\begin{pmatrix} e_{xx} & e_{xy} & e_{xz} \\ e_{yx} & e_{yy} & e_{yz} \\ e_{zx} & e_{zy} & e_{zz} \end{pmatrix} = \begin{pmatrix} e_h & 0 & 0 \\ 0 & e_h & 0 \\ 0 & 0 & e_h \end{pmatrix} + \begin{pmatrix} -e_u & 0 & 0 \\ 0 & -e_u & 0 \\ 0 & 0 & 2e_u \end{pmatrix}, \quad (\text{A4})$$

with

$$e_h = \frac{1}{3}(e_{xx} + e_{yy} + e_{zz}) = \frac{2}{3} \frac{S_{11} + 2S_{12}}{S_{11} + S_{12}} \left[\frac{a_{\parallel}}{a_0} - 1 \right], \quad (\text{A5})$$

$$e_u = \frac{1}{2}(e_{zz} - e_h) = e_h - e_{xx} = e_h - e_{yy}. \quad (\text{A6})$$

APPENDIX B

By using a Born-Haber cycle with the $Z + 1$ approximation, the core-level binding energy measured from the CVBM is expressed as Eq. (4) in the text.⁶ Here, the photoemission is treated as a process of exciting one core electron to the CVBM (the Fermi level is assumed to be at the CVBM position) and incrementing the atomic number from Z to $Z + 1$, which approximately represents the core hole in the final state.

Within the framework of tight-binding theory,^{6,19} the bond formation energy of the XAs ($X = \text{Ga, In}$) compound, $E_{\text{bond}}(XAs)$, is expressed as

$$E_{\text{bond}}(XAs) = 2E_{\text{prom}}(XAs) - 2[V_2^2(XAs) + V_3^2(XAs)]^{1/2}. \quad (\text{B1})$$

Here, $E_{\text{prom}}(XAs)$ denotes the promotion energy, $V_2(XAs)$ denotes the covalent energy, and $V_3(XAs)$ denotes the polar energy. $E_{\text{prom}}(XAs)$, $V_2(XAs)$, and $V_3(XAs)$ are given, respectively, by^{6,20}

$$E_{\text{prom}}(XAs) = \frac{1}{8}(2e_p^X - e_s^X - e_s^{\text{As}}), \quad (\text{B2})$$

$$V_2(XAs) = -3.22 \frac{\hbar^2}{md^2}, \quad (\text{B3})$$

$$V_3(XAs) = \frac{1}{2}(e_h^X - e_h^{\text{As}}). \quad (\text{B4})$$

Here, m denotes the free-electron mass, \hbar denotes the reduced Planck constant, and d denotes the bond length. e_s and e_p are the atomic s - and p -orbital energies, respectively, and $e_h^{X, \text{As}}$ is the hybrid energy, which is defined by $e_h^{X, \text{As}} = \frac{1}{4}(e_s^{X, \text{As}} + 3e_p^{X, \text{As}})$ for X and As atoms. The energy difference in E_{bond} between in the initial and final states, ΔE_{bond} , is obtained by

$$\Delta E_{\text{bond}} = 4[E_{\text{bond}}(Z+1XAs) - E_{\text{bond}}(XAs)]. \quad (\text{B5})$$

Here, $Z+1X$ denotes an atom with an atomic number of $Z + 1$.

Under an unstrained or hydrostatically strained condition, the energy position of the CVBM, E_{CV} , is given by⁶

$$E_{CV} = \frac{1}{2}(e_p^X + e_p^{\text{As}}) + \frac{1}{2} \left[\frac{1.28}{3.22} \right]^2 V_0(XAs) - \left[\left[\frac{e_p^X - e_p^{\text{As}}}{2} \right]^2 + \left[1.28 \frac{\hbar^2}{md^2} \right]^2 \right]^{1/2}, \quad (\text{B6})$$

with

$$V_0(XAs) = \frac{V_2^2(XAs)}{[V_2^2(XAs) + V_3^2(XAs)]^{1/2}}. \quad (\text{B7})$$

Here, $\frac{1}{2}(1.28/3.22)^2 V_0(XAs)$ is the nonorthogonality shift.²⁰

Metallization correction, E_{met} , represents the energy shift originating from the interaction between an X —As bond and the neighboring antibonding orbitals. To calculate the shift ΔE_{met} in the metallization correction, we have to consider the case where the X atom in an X —As bond loses an electron and also the case where the X atom in the neighboring X —As antibonds loses an electron. We then have

$$\Delta E_{\text{met}} = -4[E_{\text{met}}(XAs|O) - E_{\text{met}}(Z+1XAs|O)] - 12[E_{\text{met}}(XAs|O) - E_{\text{met}}(XAs|Z+1X)]. \quad (\text{B8})$$

Here, $E_{\text{met}}(XAs|O)$ and $E_{\text{met}}(Z+1XAs|O)$ represent the metallization energies for X —As and $Z+1X$ —As bonds, respectively, and $E_{\text{met}}(XAs|Z+1X)$ represents the metallization energy for the X —As bond next to the $Z+1X$ —As antibond.

I_{core} denotes the atomic ionization energy, which is specific to the atom species. The d dependences of ΔE_{bond} , E_{CV} , and ΔE_{met} give the energy shift in E_{CL}^{CV} . The obtained energy shift, $[E_{CL}^{CVS}(\text{theor}) - E_{CL}^{CV0}(\text{theor})]$, is -0.11 eV for the InAs strained case (type I) and 0.02 eV for the GaAs strained case (type II).

¹*Heterojunction Band Discontinuities: Physics and Device Applications*, edited by F. Capasso and G. Margaritondo (North-Holland, Amsterdam, 1987), and references cited therein.

²E. A. Kraut, R. W. Grant, J. R. Waldrop, and S. P. Kowalczyk, Phys. Rev. Lett. **44**, 1620 (1980).

³G. Osbourn, Phys. Rev. B **27**, 5126 (1983); T. Yao, Jpn. J. Appl. Phys. **23**, L521 (1983).

⁴H. Nakao and T. Yao, Jpn. J. Appl. Phys. **28**, L352 (1989).

⁵S. P. Kowalczyk, W. J. Schaffer, E. A. Kraut, and R. W. Grant, J. Vac. Sci. Technol. **20**, 705 (1982).

⁶R. Enderlein and W. A. Harrison, Phys. Rev. B **30**, 1867 (1984). Since these authors did not take into account the spin-orbit interaction, the energy position of the VBM denoted by E_{VBM} in their paper corresponds to E_{CV} in Eq. (B6).

⁷J. Menéndez, A. Pinczuk, D. J. Werder, S. K. Sputz, R. C. Miller, D. L. Sivco, and A. Y. Cho, Phys. Rev. B **36**, 8165 (1987).

⁸M. Cardona and N. E. Christensen, Phys. Rev. B **35**, 6182 (1987).

⁹C. Priester, F. Allan, and M. Lannoo, Phys. Rev. B **38**, 9870 (1988).

¹⁰A. Taguchi and T. Ohno, Phys. Rev. B **39**, 7803 (1989).

¹¹G. P. Schwartz, M. S. Hybertsen, J. Bevk, R. G. Nuzzo, J. P. Mannaerts, and G. J. Gualtieri, Phys. Rev. B **39**, 1235 (1989). In this paper, the authors calculated strain-induced shifts in the core to VBM energies in pseudomorphic Si/Ge heterostructures by the self-consistent linear-muffin-tin-orbital method. However their calculation does not take into account the XPS core-hole relaxation effect.

¹²C. G. Van de Walle and R. M. Martin, Phys. Rev. B **34**, 5621 (1986).

¹³*Landolt-Börnstein: Numerical Data and Functional Relationships in Science and Technology*, edited by O. Madelung (Springer-Verlag, Berlin, 1982).

¹⁴F. H. Pollak and M. Cardona, *Phys. Rev.* **172**, 816 (1968).

¹⁵This definition is convenient to estimate the band offsets by Eqs. (1)–(3). However, the values determined by this definition depend on the instrumental resolution, which makes it difficult to compare our values directly with the results obtained under different instrumental conditions.

¹⁶J. R. Chelicowsky and M. L. Cohen, *Phys. Rev. B* **14**, 556 (1976).

¹⁷Yu *et al.* [E. T. Yu, E. T. Croke, T. C. McGill, and R. H.

Miles, *Appl. Phys. Lett.* **56**, 569 (1990)] measured the core-level binding energies from the VBM on strained Si/Ge heterostructures.

¹⁸O. Brandt, L. Tapfer, R. Cingolani, K. Ploog, M. Hohenstein, and F. Phillipp, *Phys. Rev. B* **41**, 12 599 (1990). -

¹⁹W. A. Harrison, *Electronic Structure and the Properties of Solids* (Freeman, San Francisco, 1980).

²⁰W. A. Harrison and E. A. Kraut, *Phys. Rev. B* **37**, 8244 (1988).